

Growth rate of 3D Tetris

M.V. Tamm^{1,2}, N. Pospelov^{3,1}, and S. Nechaev^{4,5}

¹*Faculty of Physics, Lomonosov Moscow State University, 119992 Moscow, Russia*

²*Department of Applied Mathematics, MIEM, National Research University Higher School of Economics, 123458, Moscow, Russia*

³*Institute for advanced brain studies, Lomonosov Moscow State University, 119992 Moscow, Russia*

⁴*Interdisciplinary Scientific Center Poncelet (CNRS UMI 2615), 119002 Moscow, Russia*

⁵*P.N. Lebedev Physical Institute RAS, 119991 Moscow, Russia*

We consider configurational statistics of three-dimensional heaps of N pieces ($N \gg 1$) on a simple cubic lattice in a large 3D bounding box of base $n \times n$, and calculate the growth rate, $\Lambda(n)$, of the corresponding partition function, $Z_N \sim N^\theta [\Lambda(n)]^N$, at $n \gg 1$. Our computations rely on a theorem of G.X. Viennot [2], which connects the generating function of a $(D+1)$ -dimensional heap of pieces to the generating function of projection of these pieces onto a D -dimensional subspace. The growth rate of a heap of cubic blocks, which cannot touch each other by vertical faces, is thus related to the position of zeros of the partition function describing 2D lattice gas of hard squares. We study the corresponding partition function exactly at low densities on finite $n \times n$ lattice of arbitrary n , and extrapolate its behavior to the jamming transition density. This allows us to estimate the limiting growth rate, $\Lambda = \lim_{n \rightarrow \infty} \Lambda(n) \approx 9.5$. The same method works for any graph above the underlying 2D lattice and for various shapes of pieces: flat vertical squares, mapped to an ensemble of repulsive dimers, dominoes mapped to an ensemble of rectangles with hard-core repulsion, etc.

I. INTRODUCTION

We propose an estimation of the growth rate of a family of three-dimensional heaps of pieces (HP) which resemble the famous “Tetris” game on a simple cubic lattice, in which pieces of various shapes are dropped down along vertical direction until they hit already deposited elements. Formally, a heap of pieces is a collection of elementary blocks which are piled together. The main goal of the HP problem consists in computing the asymptotic behavior of the partition function, $Z_n(N) \sim N^\theta [\Lambda(n)]^N$, of all allowed distinct configurations of N -particle heaps ($N \rightarrow \infty$) in a three-dimensional bounding box with the base $n \times n$ on a lattice with a given symmetry. The critical exponent, θ , is universal and depends only on the space dimensionality, while $\Lambda(n)$ is sensitive to the lattice geometry and interaction between pieces.

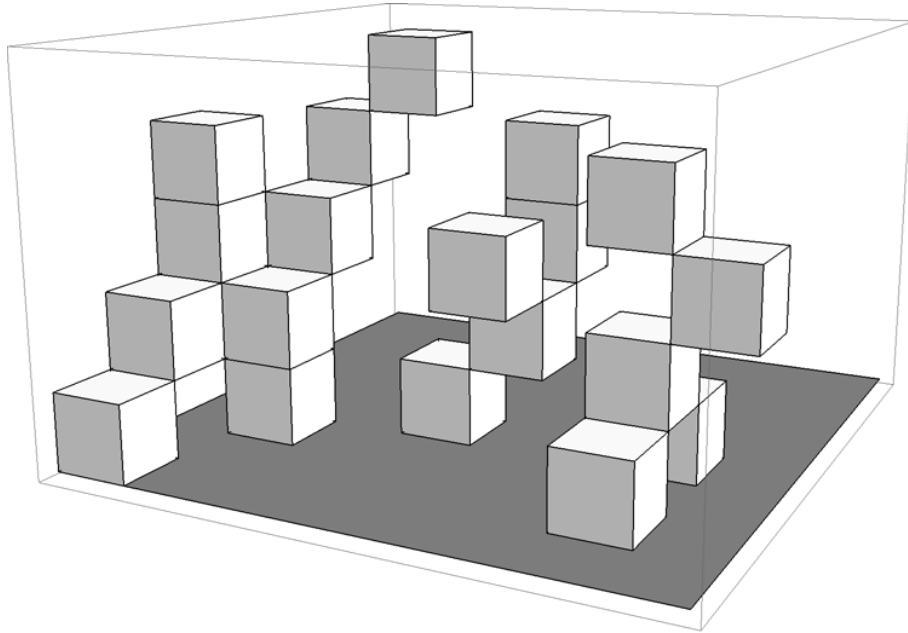


Figure 1: A typical configuration of a three-dimensional heap of cubic blocks on a simple cubic lattice.

We mostly discuss the heaps of cubic pieces which cannot touch each other by their side faces (see Fig. 1 for a typical configuration of such a heap). Although Fig. 1 is self-explanatory, it seems instructive to define the precise rules of the heap construction. Take an empty 3D bounding box with the square base (“the floor”) consisting of $n \times n$ elementary squares of size 1×1 . Add cubic blocks of size $1 \times 1 \times 1$ according to the following rules. First, distribute any number of blocks on the “floor” (with the vertical coordinate 0) in a way that blocks have no common faces (common edges are allowed). The resulting set of blocks (the first layer) we call the “roots” of the heap. Now, add new blocks to the second layer (i.e. layer with the vertical coordinate 1). The blocks of this layer must fulfil two requirements: (i) they cannot have common faces with each other, and (ii) each of them must be a nearest neighbor to one of the roots, i.e. be located either exactly on top of a root block, or have one common edge with it. Further layers are added recursively with a preceding layer regarded as a root. Thus, any block in the heap can be reached from at least one root along a *directed* path running through the collection of touching blocks (the path is called directed if it connects layers in a sequentially increasing order).

The same combinatorial problem can be posed in any dimension D and for any graph as a floor. The concept of a heap of pieces has appeared apparently for the first time in 1969 in the work of P. Cartier and D. Foata [1] where they considered monoids generated by some alphabet with the relations $ab = ba$. Various related models, as well as new combinatorial results and the relation with the statistical physics is reviewed in [2]. The 2D heaps of pieces on square and triangular lattices have been exhaustively studied in the literature and played a role of a testing ground for various approaches – from purely combinatorial [2, 11, 12], to the ones based on the diagonalization of a special transfer matrix and Bethe ansatz computations [3, 13–15].

Not much is known about the partition functions of three-dimensional heaps of pieces. To the best of our knowledge, the only one known solution of the 3D HP problem was published in 1983 by D. Dhar in [15] by an exact mapping of the HP on a body-centered-cubic lattice onto the two-dimensional hard hexagon model. The solution of the latter system has been obtained by R. Baxter using the machinery of the Bethe ansatz [16].

The HP problem met essential attention of both physicists and mathematicians. Besides the physics of growing clusters, several other problems in pure mathematics and mathematical physics are connected to the HP model. For example, various aspects [3–6] of the enumerative combinatorics of partitions are related to growth of 2D heaps of pieces. In [7] the statistics of growing heaps has been linked to the statistics of two-dimensional growing braids; in [8] the general asymptotic theory of directed two-dimensional lattice paths in half-planes and quarter-planes has been reviewed; and in [9] the algebraic ansatz for the steady-state of the totally asymmetric simple exclusion process (TASEP) on an open line has been interpreted in terms of combinatorics of 2D heaps of pieces. The discussion of algebraic approach to the ASEP model can be found in a seminal paper [10].

In our work we compute the growth rate, $\Lambda(n)$, of the ensemble of 3D heaps of cubic blocks on a simple cubic lattice in a bounding box of base $n \times n$. The growth rate $\Lambda(n)$ defines the asymptotic behavior of the partition function, $Z_n(N)$:

$$\lim_{N \rightarrow \infty} \frac{\ln Z_n(N)}{N} = \ln \Lambda(n) \quad (1)$$

Our approach relies on a beautiful relation of G. Viennot [2], that does not seem to be very widely known, and which relates the partition function of a heaps of pieces with the partition function of disposition of the projection of these pieces at the floor of the heap. We combine that relation with the semi-phenomenological analysis of zeroes of the 2D (“floor”) partition function in order to obtain an estimate for the limiting growth rate, $\Lambda = \lim_{n \rightarrow \infty} \Lambda(n)$.

II. TETRIS PARTITION FUNCTION ON A SIMPLE CUBIC LATTICE

We start with reminder of G. Viennot theorem [2], which is a keystone of our consideration. Let $Z_n(N)$ be the partition function (total number of configurations) of N -particle heap of nearest-neighbor interacting cubic blocks (see Fig. 1) inside a bounding box with $n \times n$ base, and $G_n(s)$ is the corresponding generating function (grand canonical partition function):

$$G_n(s) = \sum_{N=1}^{\infty} Z_n(N) s^N \equiv \sum_{\text{allowed configurations}} s^{\# \text{ of blocks in configuration}} \quad (2)$$

Now, consider the set of all possible roots of a heap. That is to say, we take a two-dimensional $n \times n$ square lattice, on which we distribute 1×1 squares in a way that they cannot have common sides (see Fig. 2 for a typical configuration

with $n = 6$). Let $A_{k,n}$ be the total number of configurations of k particles on the $n \times n$ -square, and $W_n(s)$ – the corresponding generating polynomial (grand partition function of a square lattice gas with the hard core repulsion):

$$W_n(s) = 1 + \sum_{k=1}^{M_{\max}} A_{k,n} s^k \quad (3)$$

by $M_{\max}(n)$ we denoted the maximal number of particles which can be arranged on a $n \times n$ lattice,

$$M_{\max} = \left[\frac{n^2 + 1}{2} \right] \quad (4)$$

31	32	33		34	35	36
25		26	27		29	30
19	20	21		22		24
	14	15			17	18
7		8	9	10	11	12
1		2	3	4	5	6

Figure 2: A configuration of 3 squares with hard-core interactions on a 6×6 square lattice. Particles are grey squares, red crosses mark the positions forbidden for the particles.

The theorem of G. Viennot states that there is a following relation between $G_n(s)$ and $W_n(s)$:

$$G_n(s) = \frac{1}{W_n(-s)} \equiv \frac{1}{1 + \sum_{k=1}^{M_{\max}} (-1)^k A_k s^k}. \quad (5)$$

Meanwhile, $Z_n(N)$ can be obtained from $G_n(s)$ in a usual way

$$Z_n(N) = \frac{1}{2\pi i} \oint \frac{G_n(s)}{s^{n+1}} ds \quad (6)$$

and, therefore, the growth rate of Z_n is simply

$$\Lambda(n) = -s_*^{-1}, \quad (7)$$

where s_* is zero of the $W_n(s)$ polynomial with the smallest absolute value.

For illustrative purposes in Appendix A we calculate $G_n(s)$ and $W_n(s)$ explicitly for $n = 2, 3$ and check directly that they do satisfy (5).

By (5) the combinatorics of 3D Tetris is reformulated as a problem of calculating the canonical partition function of the lattice “hard-square gas”, which in turn can be mapped onto the low-temperature limit of the canonical 2D Ising model on a finite square lattice in a constant magnetic field. Since exact solution of the 2D Ising model in the magnetic field is unknown, one has to rely on heuristic arguments concerning the behavior of zeroes of $W_n(-s)$, which allow us to conjecture the growth rate of the 3D heap of cubic blocks in a large bounding box (at $n \gg 1$).

We have calculated, by means of direct enumeration, all coefficients $A_{k,n}$ in (3) for $n = 2 \dots 7$, and have got the following exact explicit expressions for the polynomials $W_2(s), \dots, W_7(s)$:

$$\begin{aligned}
W_2(s) &= 1 + 4s + 2s^2; \\
W_3(s) &= 1 + 9s + 24s^2 + 22s^3 + 6s^4 + s^5; \\
W_4(s) &= 1 + 16s + 96s^2 + 276s^3 + 405s^4 + 304s^5 + 114s^6 + 20s^7 + 2s^8; \\
W_5(s) &= 1 + 25s + 260s^2 + 1474s^3 + 5024s^4 + 10741s^5 + 14650s^6 + 12798s^7 + 7157s^8 \\
&\quad + 2578s^9 + 618s^{10} + 106s^{11} + 14s^{12} + s^{13}; \\
W_6(s) &= 1 + 36s + 570s^2 + 5248s^3 + 31320s^4 + 127960s^5 + 368868s^6 + 763144s^7 + 1143638s^8 \\
&\quad + 1247116s^9 + 991750s^{10} + 576052s^{11} + 245030s^{12} + 76716s^{13} + 17834s^{14} + 3120s^{15} \\
&\quad + 416s^{16} + 40s^{17} + 2s^{18}; \\
W_7(s) &= 1 + 49s + 1092s^2 + 14690s^3 + 133544s^4 + 870589s^5 + 4216498s^6 + 15516804s^7 + 44031035s^8 \\
&\quad + 97284860s^9 + 168434824s^{10} + 229465420s^{11} + 246654832s^{12} + 209621800s^{13} + 141138510s^{14} \\
&\quad + 75497964s^{15} + 32229088s^{16} + 11059218s^{17} + 3084524s^{18} + 710124s^{19} + 137368s^{20} + 22611s^{21} \\
&\quad + 3134s^{22} + 344s^{23} + 26s^{24} + s^{25}; \tag{8}
\end{aligned}$$

As it is stated by (7), the growth rate of the 3D heap $\Lambda(n)$ is determined by the position of the root $s_*(n)$ of the polynomial $W_n(-s)$ with the smallest absolute value. In order to get some insight into the behavior of the smallest root, we have studied the roots of truncated polynomials $\bar{W}_{n,m}(-s)$, i.e., the polynomials with only m first terms preserved. The smallest root of $\bar{W}_{n,m}(-s)$ is behaving in a very peculiar way as a function of m – see Fig. 3. In Fig. 3a we draw the sequence of truncated polynomials $\bar{W}_{n,m}(-s)$ for $n = 6, 7$ and different m . One sees that for small even m the polynomials have no real roots, while for small odd m the smallest root exhibits nearly linear growth as it is shown in Fig. 3. Then, at some critical m_c a real root of the polynomial shows up for even m as well, and starting from m_c the root stabilizes, so that further increase of m does not change the root.

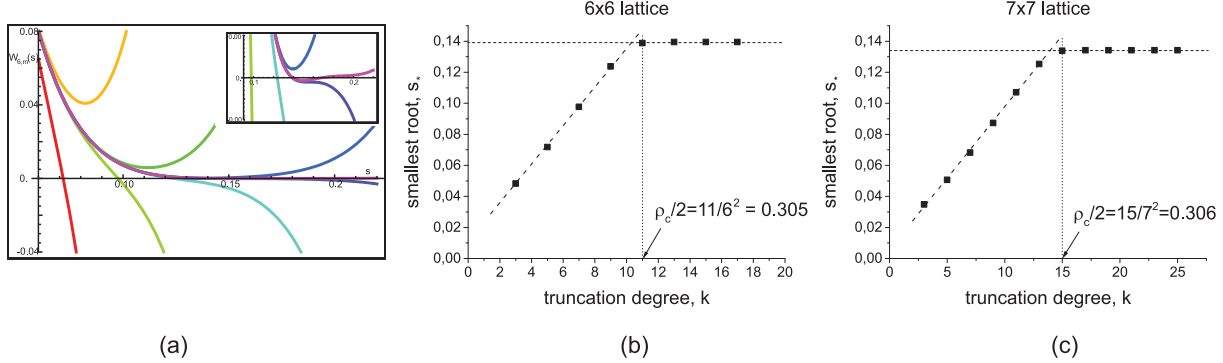


Figure 3: Behavior of smallest real roots of truncated polynomials $\bar{W}_{n,m}(-s)$: (a) truncated polynomials $\bar{W}_{6,m}(-s)$ as a function of s for $m = 5 \dots 12$ (colored from red to purple with increasing m), inset shows the vicinity of $\bar{W} = 0$; (b,c) positions of smallest real roots as a function of m for $n = 6$ (b) and 7 (c).

Based on that observation, we suggest the following heuristic procedure of estimating the value of the smallest root $s_*(n)$ on the basis of the behavior $m_c(n)$:

1. From Fig. 3b,c we expect that the fraction of occupied sites

$$\rho_c = \frac{m_c}{M_{\max}} = \frac{m_c}{\left[\frac{n^2+1}{2}\right]} \tag{9}$$

is approximately constant as a function of n . It seems reasonable to identify ρ_c with the density of ordering transition in the 2-dimensional square lattice gas with the hard-core repulsion [17, 18]. Analyzing works [17–23], one can conclude that the phase transition in the 2D hard square gas lies in the interval $0.61 < \rho_c < 0.75$, and $\rho_c \approx 0.728$ is the most probable transition value.

2. Assume some functional dependence $s_0(m)$ for $m < m_c$, where m is the truncation degree of the polynomial. It can be seen from Fig. 3b,c that the behavior is almost perfectly linear for $n = 6, 7$ (it is also true for all smaller n),

so we suggest the linear dependence

$$s_0(m|n) = A(n) + B(n) m \quad (\text{for odd } m \leq m_c) \quad (10)$$

Now, given $A(n)$ and $B(n)$ one can estimate the limiting value of the root $s_*(n)$ by substituting $m_c = \rho_c M_{\max}$ into (10). In the next section we calculate explicitly several first terms of the polynomials $W_n(s)$ for arbitrary n , which allows us to get estimates of $A(n)$ and $B(n)$ and, thus, of $s_*(n)$.

III. EVALUATION OF THE COEFFICIENTS $A_{k,n}$ FOR HARD-SQUARE LATTICE GAS

In order to evaluate the first terms in $W_n(s)$ one proceeds as follows. Enumerate the plaquettes of the $n \times n$ square lattice sequentially row-by-row as shown in Fig. 2, and introduce a $n^2 \times n^2$ “incidence” matrix T with matrix elements t_{ij} , encoding the allowed configurations of filled plaquettes. Namely,

$$t_{ij} = \begin{cases} 0 & \text{if } i = j \text{ or } i \text{ and } j \text{ are nearest neighbours} \\ 1 & \text{otherwise} \end{cases} \quad (11)$$

For example, for $n = 4$ the matrix takes form

$$T = \begin{pmatrix} 0 & 0 & 1 & 1 & 0 & 1 & 1 & 1 & 1 & 1 & 1 & 1 & 1 & 1 & 1 & 1 \\ 0 & 0 & 0 & 1 & 1 & 0 & 1 & 1 & 1 & 1 & 1 & 1 & 1 & 1 & 1 & 1 \\ 1 & 0 & 0 & 0 & 1 & 1 & 0 & 1 & 1 & 1 & 1 & 1 & 1 & 1 & 1 & 1 \\ 1 & 1 & 0 & 0 & 1 & 1 & 1 & 0 & 1 & 1 & 1 & 1 & 1 & 1 & 1 & 1 \\ 0 & 1 & 1 & 1 & 0 & 0 & 1 & 1 & 0 & 1 & 1 & 1 & 1 & 1 & 1 & 1 \\ 1 & 0 & 1 & 1 & 0 & 0 & 0 & 1 & 1 & 0 & 1 & 1 & 1 & 1 & 1 & 1 \\ 1 & 1 & 0 & 1 & 1 & 0 & 0 & 0 & 1 & 1 & 0 & 1 & 1 & 1 & 1 & 1 \\ 1 & 1 & 1 & 0 & 1 & 1 & 0 & 0 & 1 & 1 & 1 & 0 & 1 & 1 & 1 & 1 \\ 1 & 1 & 1 & 1 & 0 & 1 & 1 & 1 & 0 & 0 & 1 & 1 & 0 & 1 & 1 & 1 \\ 1 & 1 & 1 & 1 & 1 & 0 & 1 & 1 & 1 & 0 & 0 & 0 & 1 & 1 & 0 & 1 \\ 1 & 1 & 1 & 1 & 1 & 1 & 0 & 1 & 1 & 0 & 0 & 0 & 1 & 1 & 0 & 1 \\ 1 & 1 & 1 & 1 & 1 & 1 & 1 & 0 & 1 & 1 & 0 & 0 & 1 & 1 & 1 & 0 \\ 1 & 1 & 1 & 1 & 1 & 1 & 1 & 1 & 0 & 1 & 1 & 0 & 0 & 1 & 1 & 0 \\ 1 & 1 & 1 & 1 & 1 & 1 & 1 & 1 & 1 & 0 & 1 & 1 & 0 & 0 & 0 & 1 \\ 1 & 1 & 1 & 1 & 1 & 1 & 1 & 1 & 1 & 1 & 0 & 1 & 1 & 0 & 0 & 0 \\ 1 & 1 & 1 & 1 & 1 & 1 & 1 & 1 & 1 & 1 & 1 & 0 & 1 & 1 & 0 & 0 \end{pmatrix}, \quad (12)$$

where 0’s on the first subdiagonal correspond to horizontally adjacent squares (there are gaps when enumeration jumps from one raw to another), and 0’s on the fourth subdiagonal – to the vertically adjacent ones. Then for any $k \geq 1$ the coefficient $A_{n,k}$ in the expansion of $W_n(s)$, which is just the number of different ways to arrange k squares on the $n \times n$ lattice respecting the pairwise conditions encoded in the matrix T , can be formally written as follows

$$A_{n,k} = \frac{1}{k!} \sum_{i_1=1}^{n^2} \sum_{i_2=1}^{n^2} \cdots \sum_{i_k=1}^{n^2} \prod_{\alpha>\beta} t_{i_\alpha, i_\beta} \quad (13)$$

Indeed, here index i_α enumerates all possible positions of the α ’th particle, the product over all pairs of particles checks that none of them violates the nearest-neighboring restriction, and $k!$ allows for the permutations in particle enumeration.

For $k = 1$ there is no product in the equation (13), so the result is simply

$$A_{n,1} = \sum_{i=1}^{n^2} 1 = n^2 \quad (14)$$

For $k = 2$ the value $A_{n,2}$ in (13) equals to half of total number of 1’s in the matrix T , which is equal to the number of elementary white squares in the table shown in fig Fig. 4a:

$$A_{n,2} = \frac{1}{2} \sum_{i=1}^{n^2} \sum_{j=1}^{n^2} t_{ij} = \frac{n^4 - n^2 - 4(n^2 - n)}{2} = \frac{n^4 - 5n^2 + 4n}{2} \quad (15)$$

For $k = 3$ the equation (13) reads

$$A_{n,3} = \frac{1}{6} \sum_{i=1}^{n^2} \sum_{j=1}^{n^2} \sum_{k=1}^{n^2} t_{ij} t_{ik} t_{jk} \quad (16)$$

and corresponds to the enumeration of white cubes in the three-dimensional structure shown in Fig. 4b (for the $n = 4$ case). According to inclusion-exclusion principles, the sum (16) can be written as

$$A_{n,3} = \frac{1}{6} (a_0 - a_1 + a_2 - a_3), \quad (17)$$

It is easy to see that $a_0 = n^6$. One can explicitly calculate the number of black squares in Fig. 4a which is equal to $5n^2 - 4n$. Thus, $a_1 = 3n^2(5n^2 - 4n)$, where the coefficient 3 emerges from 3 unique pairs of axes: (1, 2), (2, 3), (1, 3). To obtain the terms a_2 and a_3 , we turned to the polynomial fitting. The procedure is as follows:

- (i) We explicitly calculate all a_2 and a_3 terms for 3-cubes of sizes $n = [3, 20]$. That can be done by counting the number of elementary sites with values 2 or 3 in each 3-cube. It is useful to mention that the value of an elementary site (i, j, k) in a cube is equal to the number of “improperly placed pairs” of sites on a square lattice $n \times n$.
- (ii) We fit $a_i(n)$ by a polynomial with integer coefficients. Following this procedure, we obtained the expressions: $a_2 = 3(25n^2 - 36n + 8)$, $a_3 = 13n^2 - 12n$. Collecting all coefficients, we arrive at the final result for $A_{n,3}$:

$$A_{n,3} = \frac{1}{6} (n^6 - 15n^4 + 12n^3 + 62n^2 - 96n + 24) \quad (18)$$

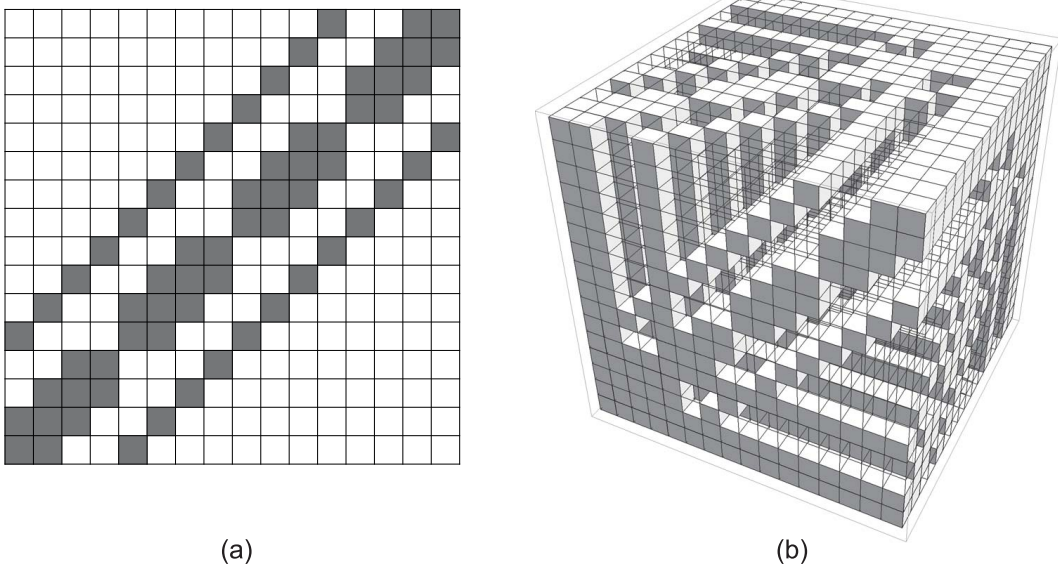


Figure 4: Counting the number of available positions of 2 and 3 hard squares in the bounding box: (a) number of 2-particle configurations is equal to empty cells in the 2D array; (b) number of 3-particle configurations is equal to number of empty cells in the shown 3D pierced structure.

We succeeded in applying such way of reasoning further for calculating $A_{n,4}$ and $A_{5,n}$. Fortunately, with the help of *Wolfram sequence solver* [24] we were able to find *On-line Encyclopedia of integer sequences* [25] and the book [26]

where on page 370 the coefficients $A_{n,k}$ are obtained for $k = 1, \dots, 9$:

$$\begin{aligned}
A_{n,1} &= n^2 \\
A_{n,2} &= \frac{1}{2}(n^4 - 5n^2 + 4n) \\
A_{n,3} &= \frac{1}{3!}(n^6 - 15n^4 + 12n^3 + 62n^2 - 96n + 24) & n \geq 2 \\
A_{n,4} &= \frac{1}{4!}(n^8 - 30n^6 + 24n^5 + 323n^4 - 504n^3 - 1110n^2 + 2760n - 1224) & n \geq 3 \\
A_{n,5} &= \frac{1}{5!}(n^{10} - 50n^8 + 40n^7 + 995n^6 - 1560n^5 - 8890n^4 + 21080n^3 + 24264n^2 - 97440n \\
&\quad + 59520) & n \geq 4 \\
A_{n,6} &= \frac{1}{6!}(n^{12} - 75n^{10} + 60n^9 + 2365n^8 - 3720n^7 - 38085n^6 + 89580n^5 + 292834n^4 - 984960n^3 \\
&\quad - 552240n^2 + 4128960n - 3160800) & n \geq 5 \\
A_{n,7} &= \frac{1}{7!}(n^{14} - 105n^{12} + 84n^{11} + 4795n^{10} - 7560n^9 - 119595n^8 + 280980n^7 + 1660204n^6 \\
&\quad - 5360880n^5 - 10985940n^4 + 52150896n^3 + 7858080n^2 - 205168320n + 187629120) & n \geq 6 \\
A_{n,8} &= \frac{1}{8!}(n^{16} - 140n^{14} + 112n^{13} + 8722n^{12} - 13776n^{11} - 309176n^{10} + 726880n^9 + 6592369n^8 \\
&\quad - 20974800n^7 - 80804780n^6 + 347456368n^5 + 445614588n^4 - 3115161504n^3 \\
&\quad + 533820336n^2 + 11725156800n - 12451057920) & n \geq 7 \\
A_{n,9} &= \frac{1}{9!}(n^{18} - 180n^{16} + 144n^{15} + 14658n^{14} - 23184n^{13} - 698040n^{12} + 1643040n^{11} \\
&\quad + 20950545n^{10} - 66240720n^9 - 395401860n^8 + 1635063696n^7 + 4294617452n^6 \\
&\quad - 24611088096n^5 - 17985223440n^4 + 208162486080n^3 - 92667609216n^2 \\
&\quad - 758613219840n + 918219939840) & n \geq 8
\end{aligned} \tag{19}$$

Thus, we are now able to write explicit expressions of all truncated polynomials for arbitrary n up to $m = 9$:

$$\overline{W}_{n,m}(s) = 1 + \sum_{k=1}^m A_{n,k} s^k \tag{20}$$

We find numerically the smallest positive roots of $\overline{W}_{n,m}(-s)$ for odd $m = 3, 5, 7, 9$ in order to estimate the values of coefficients in (10). It turns out that for all n the observed part of the dependence of the roots on m remains nearly linear. Substituting $m_c = \rho_c n^2$, where ρ_c is the critical density of the jamming transition in the 2D hard-square model, we obtain the estimate of the smallest root $s_*(n)$ of the full polynomial $W_n(-s)$.

In Fig. 5a we have demonstrated the convergence of the growth rate, $\Lambda(n) = s_*^{-1}(n)$, at $n \rightarrow \infty$ to the limiting value $\Lambda \approx 9.4$ which is evaluated at the transition density in the 2D hard square model, $\rho_c = 0.728$. In Fig. 5b we have estimated the limits within which the growth rate of the 3D heap can vary if the transition density ρ_c lies in the interval $0.61 < \rho_c < 0.75$. The limiting growth rate, Λ , in that case can vary within the interval $[\Lambda_{\min}, \Lambda_{\max}]$, where $\Lambda_{\min} = 9.28$ is evaluated at $\rho_c = 0.75$ and $\Lambda_{\max} = 11.32$ is evaluated at $\rho_c = 0.61$.

IV. DISCUSSION

In the paper we provide an estimate of the limiting growth rate, $\Lambda = \lim_{n \rightarrow \infty} \Lambda(n)$, of a partition function, $Z_N \sim N^\theta [\Lambda(n)]^N$, of 3D heaps of pieces in the large bounding box of base $n \times n$. Our estimate is based on X.G. Viennot's theorem, which establishes a relation between the grand canonical partition function of a heap $G_n(s) = \sum Z_N s^N$ and the partition function $W_n(s)$ of distributing pieces in a single layer of a heap. Namely, the theorem states that $G_n(s) = W_n^{-1}(-s)$. The limiting growth rate Λ is therefore equal to $\Lambda = \lim_{n \rightarrow \infty} s_{*,n}^{-1}$, where $s_{*,n}$ is the closest root of the polynomial $W(-s)$ with smallest absolute value.

In order to estimate the value of roots $s_{*,n}$ we studied the behavior of truncated polynomials $\overline{W}_{n,m}(-s)$, i.e. the polynomials with only first m terms preserved. We noticed that the smallest root of the truncated polynomial grows

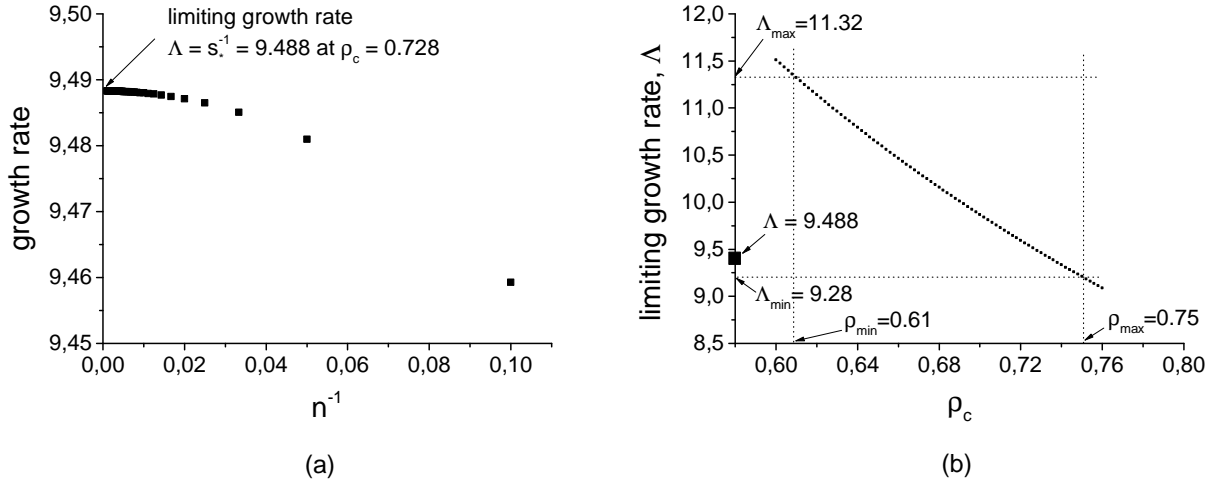


Figure 5: (a) Convergence of the growth rate, $\Lambda(n) = s_*^{-1}(n)$, at $n \rightarrow \infty$ to the limiting value $\Lambda \approx 9.5$ evaluated at $\rho_c = 0.728$; (b) Estimation of limits within which the growth rate Λ can vary if ρ_c lies in the interval $0.61 < \rho_c < 0.75$.

approximately linearly with growing m up to some critical value $m_c = \rho_c M_{\max}$, and then saturates. We estimate the linear growth rate by calculating explicitly the coefficients of the first several truncated polynomials for arbitrary n and conjecture that ρ_c coincides with the ordering transition in the 2-dimensional hard-square gas, which is the subject of a number of classical works, which provide estimates of ρ_c obtained via plenty of methods, from the perturbation theory and self-consistent approximation, to the mean-field approach and direct numeric computations, with most plausible value of critical concentration being $\rho_c \approx 0.728$. That value of ρ_c allows us to estimate the limiting growth rate of the 3D heaps as $\Lambda \approx 9.5$.

Importantly, the theorem of G.X. Viennot is valid for general heaps of pieces with arbitrary underlying graphs and arbitrary shapes the pieces. Treatment of ensembles of Tetris-like piles of heaps growing in 3D space can be straightforwardly generalized to the consideration of heaps of particles of other shapes, and even to the growth of entangled directed paths briefly described in B. Statistics of ensembles of noncrossable linear objects with topological constraints has a very broad application area ranging from self-diffusion of entangled directed polymer chains and textures of growing nanotubes, to dynamical and topological aspects of vortex glasses in high- T_c superconductors [27].

Acknowledgments

We are grateful to D. Dhar, M. Bousquet-Mélou, A. Guttmann, G. Oshainin and P. Krapivsky for valuable critique and illuminating comments, to V. Bardakov and A. Malyutin for suggestions concerning 2D extension of locally-free group, and to S. Redner for proposing the transfer matrix approach discussed in Appendix B; S.N. and N.P. acknowledge the support of the Basis Foundation No. 19-1-1-48-1.

Appendix A: Generating function of heaps of pieces in a 2×2 and 3×3 bounding boxes: transfer matrix approach

Here, in order to illustrate the statement Viennot's theorem, we calculate explicitly the generating functions $G_n(s)$ and $W_n(s)$ for $n = 2$ and 3 .

Let us construct a heap layer-by-layer ("layer" is a set of pieces of a heap with fixed vertical coordinate). In each layer the particles-squares must obey the repulsion constraint, i.e. cannot have common sides (although they can have common corners). We start with $n = 2$. The maximal possible number of particles in a layer is 2, there are 4 distinct 1-particle configurations (a particle in each of 4 corners) and 2 distinct 2-particle configurations (particles in two opposite corners). Thus,

$$W_2(s) = 1 + 4s + 2s^2 \quad (\text{A1})$$

Now, introduce vector $\mathbf{G}_{2,m}(s) = (G_{2,m}^1(s), G_{2,m}^2(s))^T$ whose components $G_{2,m}^{1(2)}(s)$ are generating functions of m -layer heaps with 1-particle (respectively, 2-particle) configuration in the upper layer. The possible configuration of m th layer depends on the state of $(m-1)$ th layer. Indeed, it is possible to put 3 different 1-particle configurations and one of the two 2-particle configurations on top of a 1-particle configurations (those which do not include the opposite corner particle), and it is possible to put any configuration on top of the two particle one. Thus, $\mathbf{G}_{2,m}(s)$ satisfies

$$\mathbf{G}_{2,m} = \mathbf{T}_2(s)\mathbf{G}_{2,m-1} \quad (\text{A2})$$

with transfer matrix

$$\mathbf{T}_2 = \begin{pmatrix} 3s & 4s \\ s^2 & 2s^2 \end{pmatrix} \quad (\text{A3})$$

and initial condition

$$\mathbf{G}_{2,1} = \begin{pmatrix} 4s \\ 2s^2 \end{pmatrix} \quad (\text{A4})$$

Thus, generating functions of heaps with arbitrary number of layers and a given configuration on top satisfy

$$\mathbf{G}_2 = \sum_{m=1}^{\infty} \mathbf{T}_2^{m-1}(s)\mathbf{G}_{2,1} = (\mathbf{I} - \mathbf{T}_2)^{-1}\mathbf{G}_{2,1}, \quad (\text{A5})$$

and the desired generating function $G_2(s)$ is

$$G_2(s) = 1 + G_2^1 + G_2^2, \quad (\text{A6})$$

where G_2^1, G_2^2 are components of \mathbf{G}_2 . Direct computation gives

$$(\mathbf{I} - \mathbf{T}_2)^{-1} = \frac{1}{1 - 3s - 2s^2 + 2s^3} \begin{pmatrix} 1 - 2s^2 & 4s \\ s^2 & 1 - 3s \end{pmatrix} \quad (\text{A7})$$

and, therefore

$$\mathbf{G}_2 = \frac{1}{1 - 3s - 2s^2 + 2s^3} \begin{pmatrix} 4s \\ 2s^2 - 2s^3 \end{pmatrix} \quad (\text{A8})$$

and

$$G_2(s) = \frac{1 + s}{1 - 3s - 2s^2 + 2s^3} = \frac{1}{1 - 4s + 2s^2}, \quad (\text{A9})$$

Thus, indeed,

$$G_2(s) = \frac{1}{W_2(-s)} \quad (\text{A10})$$

as prescribed by the Viennot's theorem.

The corresponding calculation for $n = 3$ goes exactly along the same lines but is significantly more cumbersome. Namely, there are 19 topologically different configurations of 1, 2, ..., 5 (M_{max} is 5 in this case) squares on the 3×3 lattice, as enumerated in Fig. 6. These 19 classes constitute the basis of the transfer matrix. Generally speaking, classes consist of several configurations identical up to rotation or reflection. For example, the topological class 1 in Fig. 6 represents 4 configurations of a single particle which could be located in 4 corners of the 3×3 lattice, etc. The corresponding statistical weight of each class is written above the configuration in the figure.

The generating function of a single layer, $W_3(s)$, is the sum of all weights shown in Fig. 6:

$$W_3(s) = 1 + 9s + 24s^2 + 22s^3 + 6s^4 + s^5 \quad (\text{A11})$$

(compare (8)).

The ij th element of transfer matrix, T_3 for heaps in the 3×3 bounding box enumerates the number of ways to put a layer of i -th type on top of a layer of j th type. For example, the configuration 1 in Fig. 6 can be put on top of:

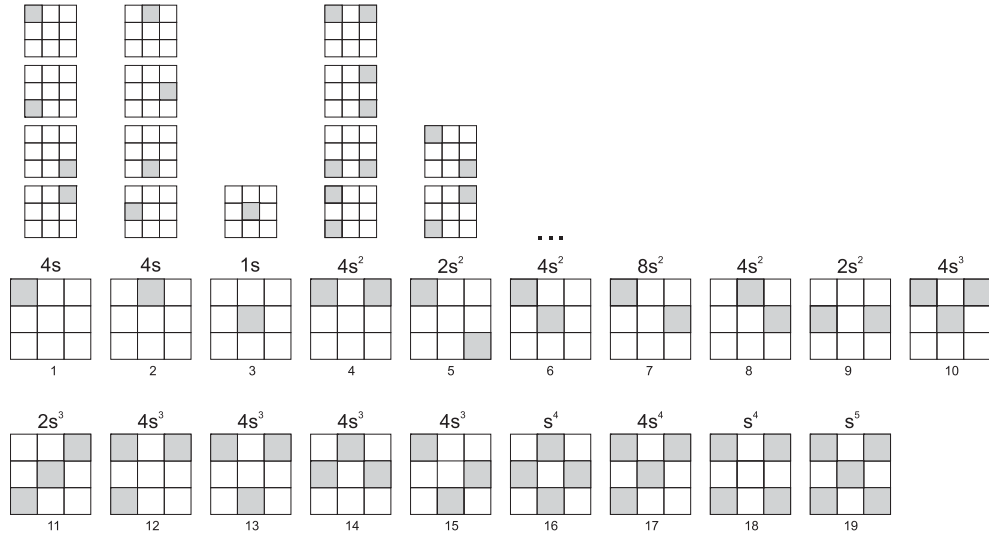


Figure 6: Enumeration of different configurations of squares with the hard-core repulsion used in the transfer matrix construction.

- 1 configuration of class 1 (the particle in the previous layer must be exactly below the particle in the current layer);
- 2 configurations of class 2 (“supporting” cube in the previous layer can be in one of the two neighboring squares, but cannot be in one of the two squares along the opposite sides of the box);
- 0 configurations of class 3 (central particle in the previous layer cannot support corner square in the current one);
- 2 configurations of class 4;
- etc

The corresponding coefficients $a_{1,1} = 1$, $a_{1,2} = 2$, $a_{1,3} = 0$, $a_{1,4} = 2, \dots$ constitute the first row of the matrix T_3 . Since class 1 consists of a single particle, the coefficients are multiplied by s^1 . Proceeding row-by-row we obtain a 19×19 transfer matrix T_3 :

$$T_{3 \times 3} = \begin{pmatrix} s & 2s & 0 & 2s & 2s & s & 3s & 3s & 4s & 2s & 2s & 3s & 4s & 4s & 4s & 3s & 4s & 4s \\ 2s & s & 4s & 3s & 4s & 4s & 3s & 2s & 2s & 4s \\ 0 & s & s & 0 & 0 & s & s & s & s & s & s & 0 & s & s & s & s & s & 0 & s \\ 0 & s^2 & 0 & s^2 & 0 & 0 & 2s^2 & 2s^2 & 4s^2 & s^2 & 0 & 2s^2 & 4s^2 & 4s^2 & 4s^2 & 2s^2 & 4s^2 & 4s^2 \\ 0 & 0 & 0 & 0 & s^2 & 0 & s^2 & s^2 & 2s^2 & 0 & s^2 & s^2 & 2s^2 & 2s^2 & 2s^2 & s^2 & 2s^2 & 2s^2 \\ 0 & 2s^2 & 0 & 0 & 0 & s^2 & 3s^2 & 3s^2 & 4s^2 & 2s^2 & 2s^2 & 0 & 4s^2 & 4s^2 & 4s^2 & 3s^2 & 0 & 4s^2 \\ 0 & 0 & 0 & 2s^2 & 4s^2 & 2s^2 & 4s^2 & 2s^2 & 4s^2 & 4s^2 & 6s^2 & 8s^2 & 6s^2 & 8s^2 & 8s^2 & 6s^2 & 8s^2 & 8s^2 \\ s^2 & 0 & 4s^2 & 2s^2 & 4s^2 & 2s^2 & s^2 & 0 & 4s^2 & 4s^2 & 4s^2 & 2s^2 & 4s^2 & 4s^2 & 4s^2 & 4s^2 & 4s^2 & 4s^2 \\ 0 & 0 & 2s^2 & s^2 & 2s^2 & 2s^2 & s^2 & 0 & s^2 & 2s^2 \\ 0 & s^3 & 0 & 0 & 0 & 0 & 2s^3 & 2s^3 & 4s^3 & s^3 & 0 & 0 & 4s^3 & 4s^3 & 4s^3 & 4s^3 & 2s^3 & 0 & 4s^3 \\ 0 & 0 & 0 & 0 & 0 & 0 & s^3 & s^3 & 2s^3 & 0 & s^3 & 0 & 2s^3 & 2s^3 & 2s^3 & 2s^3 & s^3 & 0 & 2s^3 \\ 0 & 0 & 0 & 0 & 0 & 0 & s^3 & s^3 & 4s^3 & 0 & 0 & s^3 & 4s^3 & 4s^3 & 4s^3 & s^3 & 4s^3 & 4s^3 & 4s^3 \\ 0 & 0 & 0 & 0 & 0 & 0 & s^3 & 0 & 2s^3 & s^3 & 0 & 2s^3 & 4s^3 & 3s^3 & 4s^3 & 4s^3 & 2s^3 & 4s^3 & 4s^3 \\ 0 & 0 & 4s^3 & s^3 & 4s^3 & 4s^3 & s^3 & 0 & 0 & 4s^3 & 4s^3 & 4s^3 & s^3 & 4s^3 & 4s^3 & 4s^3 & 4s^3 & 4s^3 & 4s^3 \\ 0 & 0 & 0 & 0 & 2s^3 & s^3 & s^3 & 0 & 0 & 2s^3 & 2s^3 & 3s^3 & 4s^3 & 2s^3 & 4s^3 & 4s^3 & 3s^3 & 4s^3 & 4s^3 \\ 0 & 0 & s^4 & 0 & s^4 & s^4 & 0 & 0 & 0 & s^4 & s^4 & s^4 & s^4 & 0 & s^4 & s^4 & s^4 & s^4 & s^4 \\ 0 & 0 & 0 & 0 & 0 & 0 & s^4 & s^4 & 4s^4 & 0 & 0 & 0 & 4s^4 & 4s^4 & 4s^4 & s^4 & 0 & 4s^4 \\ 0 & 0 & 0 & 0 & 0 & 0 & 0 & s^4 & 0 & 0 & 0 & s^4 & s^4 & s^4 & s^4 & 0 & s^4 & s^4 \\ 0 & 0 & 0 & 0 & 0 & 0 & 0 & s^5 & 0 & 0 & 0 & s^5 & s^5 & s^5 & s^5 & 0 & 0 & s^5 \end{pmatrix} \quad (A12)$$

Now, similarly to the $n = 2$ case the partition function of the heap is

$$G_3(s) = 1 + \sum_{l=1}^{19} G_3^{(l)} \quad (A13)$$

where $G_3^{(l)}$ are elements of the vector

$$\mathbf{G}_3(s) = (\mathbf{I} - \mathbf{T}_3)^{-1} \mathbf{G}_{3,1}(s) \quad (\text{A14})$$

and $\mathbf{G}_{3,1}(s) = (4s, 4s, s, 4s^2, 2s^2, 4s^2, 8s^2, 4s^2, 2s^2, 4s^3, 2s^3, 4s^3, 4s^3, 4s^3, 4s^3, s^4, 4s^4, s^4, s^5)^\top$ is the generating vector of 1-layer heaps. It is easy to evaluate (A13)–(A14) using symbol calculation software and find that, indeed,

$$G_3(s) = \frac{1}{1 - 9s + 24s^2 - 22s^3 + 6s^4 - s^5} = \frac{1}{W_3(-s)}. \quad (\text{A15})$$

Appendix B: Statistics of entangled (2+1)D braids

The system shown in Fig. 7a describes the collective dynamics of random directed paths in (2+1)D and ultimately leads to the consideration of a (2+1)D "surface" braid group B_n^{2D} . Following [28], consider the two-dimensional lattice Z^2 and enumerate its vertices sequentially line-by-line: P_1, P_2, \dots, P_{n^2} . A (2+1)D-braid of n^2 directed strings on Z^2 based at $\{P_1, \dots, P_{n^2}\}$ is an n^2 -tuple $b = (b_1, \dots, b_{n^2})$ of paths, such that:

- (i) $b_i(1) = P_i$ for $i \in \{1, \dots, n^2\}$;
- (ii) $b_i(t) \neq b_j(t)$ for all $\{i, j\} \in \{1, \dots, n^2\}$, $(i \neq j, t \in [1, N])$. The surface braid group B_n^{2D} is the group of homotopy classes of braids based at $\{P_1, \dots, P_{n^2}\}$. The group B_n^{2D} has generators $\sigma_{ij}^{(x)}, \sigma_{ij}^{(y)}$, $(i, j) \in \{1, \dots, n\}$ and their inverses with the standard braiding relations [28].

The geometric representation of generators of B_n^{2D} is shown in Fig. 7b.

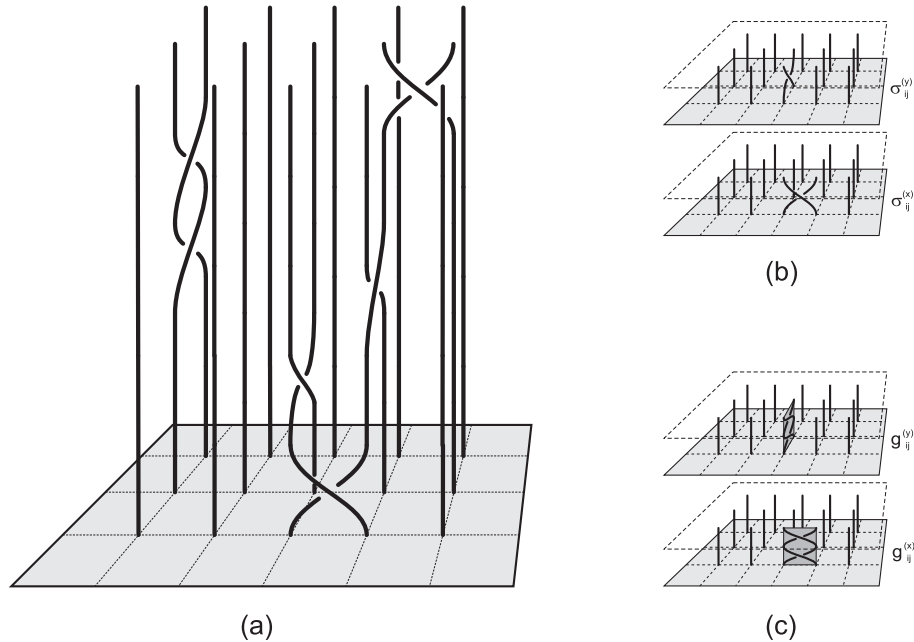


Figure 7: (a) Schematic picture of the surface braid in (2+1)D space; (b) surface braid group generator; (c) generator of the "surface locally free group".

Define now a symmetric random walk on a set of generators ("blocks") $\{\sigma_{11}^{(x)}, \sigma_{11}^{(y)}, \dots\}$ with the uniform probability $\frac{1}{n^2}$. This random walk can be viewed as a random uniform "ballistic deposition" when we add sequentially new blocks to the roof of a growing heap. One of keynote questions in statistics of entangled lines concerns the evaluation of a number of all nonequivalent topological states after adding N braid group generators. This challenging problem is yet unsolved, however some reasonable estimates can be obtained using the concept of the so-called *surface locally free group* [7]. The (2+1)D ("surface") locally free group \mathcal{LF}_{n-1}^{2D} is constructed on the basis of the braid group B_n^{2D}

by omitting the braiding relations. The group \mathcal{LF}_{n-1}^{2D} has generators $g_{ij}^{(x)}, g_{ij}^{(y)}$, where $(i, j) \in \{1, \dots, n\}$, with the following commutation relations (compare Fig. 7c and Fig. 8b):

$$\begin{cases} g_{i_1, j_1}^{(x)} g_{i_2, j_2}^{(x)} = g_{i_2, j_2}^{(x)} g_{i_1, j_1}^{(x)} \quad (|j_1 - j_2| > 0 \text{ or } |i_1 - i_2| > 1) \\ g_{i_1, j_1}^{(x)} g_{i_2, j_2}^{(y)} = g_{i_2, j_2}^{(y)} g_{i_1, j_1}^{(x)} \quad (i_2 - i_1 \text{ or } j_1 - j_2) \neq \{0, 1\} \\ g_{i,j}^{(x)} (g_{i,j}^{(x)})^{-1} = g_{i,j}^{(y)} (g_{i,j}^{(y)})^{-1} = e \end{cases} \quad (\text{B1})$$

It can be proven that $g_{ij}^{(x)} = (\sigma_{ij}^{(x)})^2$ and $g_{ij}^{(y)} = (\sigma_{ij}^{(y)})^2$. There is a bijection between words in locally free group and *colored heaps*, whose elements are either “white” $g_{ij}^{(x,y)}$ or “black” $(g_{ij}^{(x,y)})^{-1}$. That is, any word written in terms of letters–generators of the group \mathcal{LF}_n^{2D} represents an unique configuration of a colored heap (see Fig. 8a) in a box of base of $n \times n$ and vice versa: any heap uniquely defines some word in the group \mathcal{LF}_n^{2D} . The configuration of the heap with a black block following immediately after a white one in the same column is forbidden. The process of a heap’s growth consists in adding step-by-step new blocks to the roof. The typical configuration of a heap is shown in Fig. 8a.

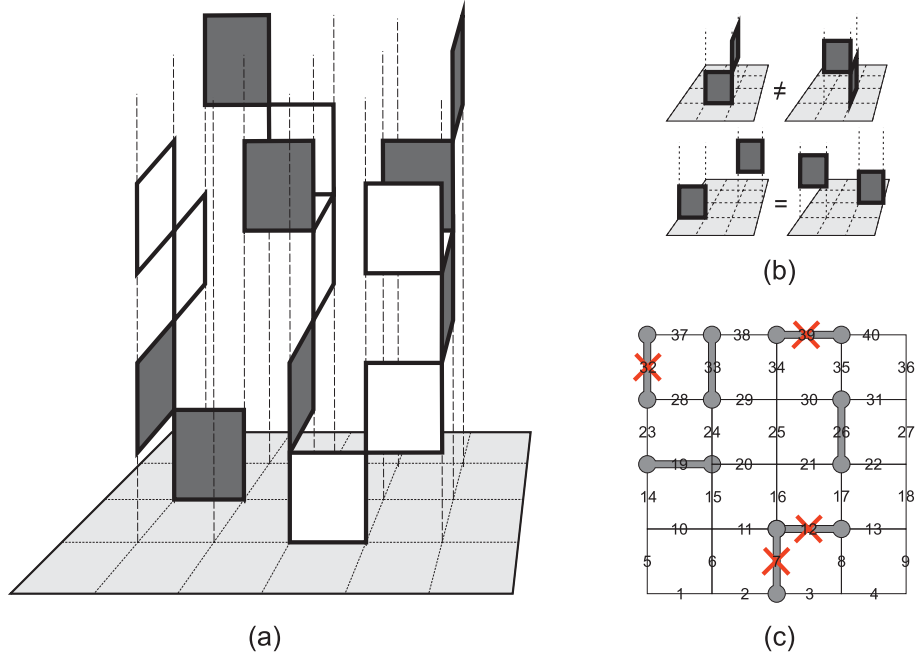


Figure 8: (a) Heap consisting of interacting vertically oriented squares. Enumeration of such heaps provides the upper estimate for the number of topologically different configurations of surface braids; (b) generators of surface locally-free group (same as in Fig. 7b); (c) projection of pieces constituting heap to the base plane gibes the collection of dimers with hard core interactions (red crossed demonstrate forbidden configurations).

Thus, the problem of estimating from above the number of different topological states of randomly entangled lines is reformulated as the problem of evaluating the number of different configurations (i.e. the partition function) of a heap raised of N elementary vertical squares representing generators $g_{ij}^{(x)}$ or $g_{ij}^{(y)}$ – see Fig. 8a and Fig. 8b. To compute the growth of the heap of such pieces, we can use again the relation between generating function of heaps and 2D projection of pieces to the base plane, which are dimers in that case. Thus, we can apply the whole machinery developed for a gas of hard squares to the systems of hard-core interacting dimers on a square lattice (see Fig. 8c) and estimate the growth rate of heap of flat squares in 3D. That will enable us to estimate from above the number of different topological states of randomly entangled directed lines in (2+1)D. We expect to realize the corresponding

program in the forthcoming publication.

[1] P. Cartier and D. Foata, Problèmes combinatoires de commutation et réarrangements, Lecture Notes in Mathematics (Springer-Verlag: New-York/Berlin), **85** 1969

[2] G.X. Viennot, Heaps of pieces, I : Basic definitions and combinatorial lemmas, in: Labelle G., Leroux P. (eds) Combinatoire énumérative, Lecture Notes in Mathematics, (Springer: Berlin, Heidelberg), **1234** 321 (1993)

[3] V. Hakim and J.P. Nadal, Exact results for 2D directed animals on a strip of finite width, *J. Phys. A: Math. Gen.* **16** L213 (1983)

[4] D. Gouyou-Beauchamps and G.X. Viennot, Equivalence of the Two-Dimensional Directed Animal Problem to a One-Dimensional Path Problem, *Adv. Appl. Math.* **9** 334 (1988)

[5] M. Bousquet-Mélou, New enumerative results on two-dimensional directed animals, *Discrete Mathematics* **180** 73 (1998)

[6] M. Bousquet-Mélou and A. Rechnitzer, Lattice animals and heaps of dimers, *Discrete Mathematics* **258** 235 (2002)

[7] A. M. Vershik, S. Nechaev and R. Bikbov, Statistical Properties of Locally Free Groups with Applications to Braid Groups and Growth of Random Heaps, *Comm. Math. Phys.* **212**, 469 (2000)

[8] C. Banderier, Ph. Flajolet, Basic analytic combinatorics of directed lattice paths, *Theoretical Computer Science*, **281** 37 (2002)

[9] N. Haug, S. Nechaev, M. Tamm, From generalized directed animals to the asymmetric simple exclusion process, *J. Stat. Mech. P-10013* (2014)

[10] B. Derrida, M.R. Evans, V. Hakim, and V. Pasquier, Exact solution of a 1D asymmetric exclusion model using a matrix formulation. *J. Phys. A: Math. Gen.* **26** 1493 (1993)

[11] J. Bétrêma and J.G. Penaud, Modèles avec particules dures, animaux dirigés, et séries en variables partiellement commutatives, ArXiv:math/0106210

[12] M. Bousquet-Mélou and R. Brak, Exactly solved models of polyominoes and polygons, arXiv:0811.4415

[13] D. Dhar, M.K. Phani, and M. Barma, Enumeration of directed site animals on two-dimensional lattices, *J. Phys. A* **15** L279 (1982)

[14] Equivalence of the Two-Dimensional Directed-Site Animal Problem to Baxter's Hard-Square Lattice-Gas Model, *Phys. Rev. Lett.* **49** 959 (1982)

[15] D. Dhar, Exact Solution of a Directed-Site Animals – Enumeration Problem in Three Dimensions, *Phys. Rev. Lett.* **51** 853 (1983)

[16] R.J. Baxter, Hard hexagons: exact solution, *J. Phys. A: Math. Gen.* **13** L61 (1980)

[17] D.M. Burley, A Lattice Model of a Classical Hard Sphere Gas: II, *Proc. Phys. Soc.* **77** 451 (1961)

[18] D. S. Gaunt and M. E. Fisher, HardSphere Lattice Gases. I. PlaneSquare Lattice, *J. Chem. Phys.* **43**, 2840 (1965)

[19] L.K. Runnels and L.L. Coombs, Exact Finite Method of Lattice Statistics. I. Square and Triangular Lattice Gases of Hard Molecules, *J. Chem. Phys.* **45** 2482 (1966)

[20] R. J. Baxter, I. G. Enting, and S. K. Tsang, Hard-square lattice gas, *J. Stat. Phys.* **22**, 465 (1980); R. J. Baxter, Planar lattice gases with nearest-neighbor exclusion, *Ann. Combin.* **3**, 191 (1999)

[21] G. Kamieniarz and H.W.J. Blöte, The non-interacting hard-square lattice gas: Ising universality, *J. Phys. A: Math. Gen.* **26** (1993) 6679

[22] A. Baram and M. Fixman, Hard square lattice gas, *J. Chem. Phys.* **101** 3172 (1994)

[23] H.C. Marques Fernandes, Y. Levin, and J.J. Arenzon, Equation of state for hard square lattice gases, *Phys. Rev. E* **75** 052101 (2007)

[24] Wolfram sequence solver, <https://www.wolframalpha.com/>

[25] The On-Line Encyclopedia of Integer Sequences (OEIS), <https://oeis.org/>

[26] Václav Kotěšovec, Non-attacking chess pieces (chess in mathematics), 6th edition, http://www.koteshovec.cz/books/koteshovec_non_attacking_chess_pieces_2013_6ed.pdf

[27] D.R. Nelson, Vortex Entanglement in High- T_c Superconductors, *Phys. Rev. Lett.* **60** 1973 (1988); D.R. Nelson, H. Seung, Theory of melted flux liquids, *Phys. Rev. B* **39** 9153 (1989)

[28] J. Birman, Mapping class groups of surfaces, *Contemp. Math.* **78** 13 (1988)